Turbulent Forced Convection Flow in a Channel over Periodic Grooves using Nanofluids

Farshid Fathinia, Mohammad Parsazadeh, and Amirhossein Heshmati

Abstract—Turbulent forced convection flow in a 2-dimensional channel over periodic grooves is numerically investigated. Finite volume method is used to study the effect of turbulence model. The range of Reynolds number varied from 10000 to 30000 for the rib-height to channel-height ratio (B/H) of 2. The downstream wall is heated by a uniform heat flux while the upstream wall is insulated. The investigation is analyzed with different types of nanoparticles such as SiO_2, Al_2O_3, and ZnO, with water as a base fluid are used. The volume fraction is varied from 1% to 4% and the nanoparticle diameter is utilized between 20nm to 50nm. The results revealed 114% heat transfer enhancement compared to the water in a grooved channel by using SiO_2 nanoparticle with volume fraction and nanoparticle diameter of 4% and 20nm respectively.

Keywords—Forced convection, Periodic grooves, Nanofluids, Turbulent model, Heat transfer.

I. INTRODUCTION

THE improvement of heat transfer has been paid more attention due to increasing the engineering applications. One of the common passive ways to enhance the heat transfer is using the roughen surfaces, grooves, baffles, and ribs to produce local turbulent flow or disturbing the flow.

High performance of various engineering applications is owed to the efficient heat transfer enhancement. Grooved channels have a significant role in this sort of heat transfer enhancement. Energy system equipment, electronic cooling, cooling of nuclear reactors, cooling of turbine blades, combustion chambers, environmental control systems are the beneficial samples of this method [1].

Analyzing the thermal and flow field over groove channel has been experimentally and numerically done by investigators since last two decades. Eiamsa and Promvonge [2] have investigated flow and thermal behavior of forced convection of an incompressible airflow in a 2-dimensional channel with 9 periodic transverse grooves on its lower wall. They found that reverse re-circulation flow can considerably increase heat transfer in a transverse grooves channel.

Adachi et al. [3] presented the effect of expanded grooves on pressure drop determined in a horizontal channel including

F. Fathinia is with the Faculty of Mechanical Engineering, Universiti Teknologi Malaysia, 81310 UTM Johor Bahru, Malaysia (phone: +60-172029501; e-mail: ffarshid2@ live.utm.my).
M. Parsazadeh is with the Faculty of Mechanical Engineering, Universiti Teknologi Malaysia, 81310 UTM Johor Bahru, Malaysia (phone: +60-1761885368; e-mail: pmohammad4@ live.utm.my).
A.H.Heshmati is with the Faculty of Mechanical Engineering, Universiti Teknologi Malaysia, 81310 UTM Johor Bahru, Malaysia (phone: +60-173818348; e-mail: hamirhossein2@ live.utm.my).

54 grooves sets to measure the pressure drop even for small Reynolds numbers. Adachi and Uehara [4] studied Correlation between heat transfer and pressure drop in 2-dimensional horizontal channels using fully developed flow with periodically grooved parts.

A considerable effect on heat transfer was seen by changing rib shapes. Rib-Triangular groove (RR-TG), Triangular rib-Triangular groove (TR-TG) and Triangular rib-Rectangular groove (TR-RG) were three shapes that having mounted on the lower wall of channel and analyzed with a turbulent flow by Eiamsa and Promvonge [5]. They found that Rectangular rib-Triangular groove (RR-TG) has highest heat transfer. They also studied the effects of pitch ratio on heat transfer rate for these three geometries. In a similar effort Kamali and Binesh [6] studied effects of square, trapezoidal and triangular rib shapes with decreasing height, while increasing height was in trapezoidal rib shape numerically, on characteristics of turbulent incompressible airflow in a 2-dimensional horizontal ribbed channel, while uniform heat flux was imposed on lower wall and upper wall was maintained in an adiabatic condition. They concluded the highest mean Nusselt number and enhancement factor were for trapezoidal rib with decreasing height. Effects of Reynolds number and wall thermal conductivity ratio to the fluid and geometric parameters on heat transfer for rectangular and arc-shaped grooves have been reported by Shokouhmand et al. [7]. Heat transfer in an intermittently and symmetrically grooved channel with 7 contiguous triangular grooves followed by a flat section in the range of Reynolds number varying between 600 and 1,800 was investigated by Greiner et al. [8]. Their results revealed that Nusselt number is went up with increasing Reynolds number.

As for flow characteristics effects, modifying the topology of grooved channel is another way to increase the heat transfer, having been utilized by researchers during last decades. Herman and Kang [9] experimentally studied forced convection cooling of electrical components in grooved channels with three different topologies of basic grooved channel (BGC), grooved channel with cylindrical eddy promoters (GCC) and grooved channel with curved vanes (GCV) in laminar, transitional and turbulent airflows in the range of 200 to 6,500 Reynolds number. They reported BGC is the best for moderate to high Reynolds numbers while GCV has the optimum performance. They also investigated the heat transfer performance of grooved channel by attaching curved vanes at downstream of each block. The goal of using curved vanes in this experiment was to enhance heat transfer at flank

World Academy of Science, Engineering and Technology
International Journal of Mechanical and Mechatronics Engineering
Vol:6, No:12, 2012

regions and eliminate large recirculation zone in grooves. Ortiz et al. [10] have investigated the heat transfer enhancement in a 2-dimensional horizontal grooved channel by attaching curved deflectors. They revealed that in basic grooved channels; flow after passing over a rib directly hits the next rib, is heated, gets trapped and creates recirculation flow.

Some researchers have focused on utilizing nanofluids to increase heat transfer parameters. Oronzio et al. [11] studied the effect of nanofluids on ribbed channel numerically and found that heat transfer is improved. Al-aswadi et al. [12] investigated numerically forced convection flow over backward facing step by using nanofluids. In their research water was base fluid and Au, Ag, Cu, CuO, Al$_2$O$_3$, SiO$_2$, TiO$_2$, and diamond were nanoparticles. They concluded SiO$_2$ have generally improved the heat transfer.

It is clear from above studies that conventional fluids have been used to investigate the characteristics of heat transfer and using nanofluids flow was not analyzed on grooved channel and it has motivated the current study. In the present study, 2-dimentional numerical simulations over periodic grooves in a horizontal channel are carried out using various nanofluids (SiO$_2$, Al$_2$O$_3$, and ZnO) with volume fraction and nanoparticle diameter of 1-4% and 20-50nm respectively. Water has been chosen as the base fluid under study. The purpose of this study is to obtain the Nusselt number and friction factor along the channel for choosing the best nanoparticle and having the most heat transfer enhancement.

II. MODEL DESCRIPTION AND GOVERNING EQUATIONS

The schematic of interested system is shown in Fig. 1. This channel was fixed by nine grooves and 8 ribs along the downstream channel wall. The channel length, rib land (s) is set to be 1870 mm and 5H/4 respectively. The channel height is H=40mm, while groove width (B) is fixed to 3H/4. The entry length of 20H is considered to create a fully developed flow. The last groove is located to 10H upstream of the exit. The length of test section and rib height was 670 mm and H/2 mm, respectively. This geometry has been fixed by eight ribs with the length of 50mm (s=5H/4). The groove width ratio, (B/H), is located to be B/H=0.75. Foregoing geometrical dimensions and heat flux are the same as grooved channel of smith and Pongjet [2].
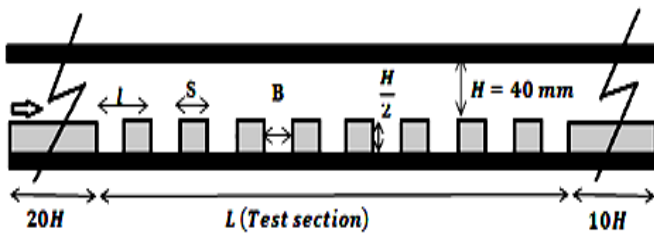

Fig. 1 Grooved channel

TABLE I
NOMENCLATURE

Symbol	Quantity
B	distance between grooves
C_μ	turbulence model constant
D_h	hydraulic diameter of channel
e	rib height or groove depth
f	friction factor
H	channel height
h	convective heat transfer coefficient
k	thermal conductivity
L	channel length of test section
Nu	Nusselt number
p	static pressure
Ra	Reynolds number
s	rib land/length
T	temperature
U	mean velocity
u'_i	fluctuation velocity components
μ	kinematic viscosity
μ_t	eddy viscosity
τ_{ij}	Reynolds stress
τ	wall shear stress
n	thermal enhancement factor
ω	turbulent specific dissipation rate
ε	turbulent dissipation rate
ρ	density
TKE	turbulent kinetic energy
l	groove and rib land

The governing equations under consideration of the steady 2-dimensional incompressible form of Continuity equation, Navier-Stokes equations and Energy equation are as [2]:

Continuity equation:

$$\frac{\partial}{\partial x_i}(\rho u_i) = 0 \qquad (1)$$

Momentum equation:

$$\frac{\partial(\rho u_i u_j)}{\partial x_i} = -\frac{\partial p}{\partial x_i} + \frac{\partial}{\partial x_i}\left[\mu\left(\frac{\partial u_i}{\partial x_j} + \frac{\partial u_j}{\partial x_i}\right) + \frac{\partial}{\partial x_i}\left(-\rho\overline{u_i' u_j'}\right)\right] \qquad (2)$$

Energy equation:

$$\frac{\partial}{\partial x_i}(\rho u_i T) = \frac{\partial}{\partial x_j}(\Gamma + \Gamma_t)\frac{\partial \tau}{\partial x_j} \qquad (3)$$

where Γ and Γ_t in energy equation are molecular thermal diffusivity and turbulent thermal diffusivity respectively have been given as:

$$\Gamma = \frac{\mu}{Pr} \text{ and } \Gamma_t = \frac{\mu_t}{Pr_t} \qquad (4)$$

World Academy of Science, Engineering and Technology
International Journal of Mechanical and Mechatronics Engineering
Vol:6, No:12, 2012

The K-ε turbulence model is chosen for modeling Reynolds stresses $\left(-\rho\overline{u_i' u_j'}\right)$ in eq. (2). The boussinesq hypothesis is used to relate Reynolds stresses to mean velocity gradient:

$$\left(-\rho\overline{u_i' u_j'}\right) = \mu_t \left(\frac{\partial u_i}{\partial x_j} + \frac{\partial u_j}{\partial x_i}\right) \qquad (5)$$

The k-ε model is one of the most common turbulence models including two extra transport equations to represent the turbulent properties of the flow. The two transport variables are turbulent kinetic energy, K and the turbulent dissipation, ε. The k-ε turbulence model has three types including Standard k-ε model, Realizable k-ε model and RNG k-ε model. In the present study, the RNG k-ε model is utilized in order to validation of mentioned model was being consistent with experimental results in Smith and Pongjet study [2].

The turbulence viscosity is given by:

$$\mu_t = \rho C_\mu \frac{k^2}{\varepsilon} \qquad (6)$$

The modeled turbulent kinetic energy is written as:

$$\frac{\partial}{\partial x_i}(\rho K u_i) = \frac{\partial}{\partial x_j}\left[\left(\mu + \frac{u_t}{\sigma_k}\right)\frac{\partial k}{\partial x_j}\right] + G_k - \rho\varepsilon \qquad (7)$$

The dissipation rate of TKE, ε, is similarly given by:

$$\frac{\partial}{\partial x_i}(\rho\varepsilon u_i) = \frac{\partial}{\partial x_j}\left[\left(\mu + \frac{u_t}{\sigma_k}\right)\frac{\partial \varepsilon}{\partial x_j}\right] + C_{1\varepsilon}\frac{\varepsilon}{k}G_k - C_{2\varepsilon}\rho\frac{\varepsilon^2}{k} \qquad (8)$$

where G_k is the rate of generation of the TKE while $\rho\varepsilon$ is its destruction rate. G_k is given by:

$$G_k = -\rho\overline{u_i' u_j'}\frac{\partial u_j}{\partial x_i} \qquad (9)$$

Constants used in k-ε model are chosen to be empirical constants [2]. C_{1t}=1.44. C_{2t}=1.92, C_μ=1.44, σ_t=1.3, σ_k=1, and pr_t=0.9.

The density of nanofluid can be obtained from [13]:

$$\rho_{nf} = (1-\phi)\rho_f + \phi\rho_{np} \qquad (10)$$

where ρ_f and ρ_{np} are mass densities of base fluid and NPs, respectively.

The effective heat capacity is given as [13]:

$$\left(\rho C_p\right)_{nf} = (1-\phi)\left(\rho C_p\right)_f + \phi\left(\rho C_p\right)_{np} \qquad (11)$$

where $(\rho C_p)_f$ and $(\rho C_p)_{np}$ are heat capacities of base fluid and Nanoparticles, respectively.

The effective thermal conductivity equation of nanofluid is written as [13]:

$$k_{eff} = k_{static} + k_{Brwnian} \qquad (12a)$$

$$k_{static} = k_f\left[\frac{(k_{np}+2k_f) - 2\phi(k_f - k_{np})}{(k_{np}+2k_f) + \phi(k_f - k_{np})}\right] \qquad (12.b)$$

$$k_{Brwnian} = 5\times10^4 \beta\phi\rho_f C_{p,f}\sqrt{\frac{KT}{2\rho_{np}R_{np}}}f(T,\phi) \qquad (12.c)$$

where K_{np} and K_f are the thermal conductivities of nanoparticles and base fluid respectively.

Boltzman Constant:

$$k = 1.3807\times10^{-23}\ {}^{J}\!/\!{}_{K} \qquad (12.d)$$

$$f(T,\phi) = \left(2.8217\times10^{-2}\phi + 3.917\times10^{-2}\right)\left(\frac{T}{T_0}\right)$$
$$+ \left(-3.0669\times10^{-2}\phi - 3.391123\times10^{-2}\right) \qquad (12.e)$$

for $1\% \leq \phi \leq 4\%$ and 300K , where T is the fluid temperature, and T_0 is the reference temperature.

The effective viscosity can be obtained using following mean empirical correlations [13]:

$$\mu_{eff} = \mu_f \times \frac{1}{\left(1 - 34.87\left(d_p/d_f\right)^{-0.3}\times\varphi^{1.03}\right)} \qquad (13a)$$

$$d_f = \left[\frac{6M}{N\pi\rho f_0}\right]^{\frac{1}{3}} \qquad (13.b)$$

where M is the molecular weight of base fluid, N is the Avogadro number, and ρ_{f0} is the mass density of the based fluid calculated at temperature T_0=293K.

The effective thermal expansion is expressed as [13]:

$$\left(\rho\beta\right)_{nf} = (1-\phi)\left(\rho\beta\right)_f + \phi\left(\rho\beta\right)_{np} \qquad (14)$$

for different particle materials the β equations are listed in Table II.

World Academy of Science, Engineering and Technology
International Journal of Mechanical and Mechatronics Engineering
Vol:6, No:12, 2012

TABLE II
β VALUES FOR DIFFERENT PARTICLES

Type of particles	β	Concentration (%)
SiO_2	$1.9526(100\phi)^{-1.4594}$	$1\% \leq \varphi \leq 10\%$
Al_2O_3	$8.4407(100\phi)^{-1.07304}$	$1\% \leq \varphi \leq 6\%$
ZnO	$8.4407(100\phi)^{-1.07204}$	$1\% \leq \varphi \leq 7\%$

III. NUMERICAL IMPLEMENTATION

Governing equations is solved by finite volume method using SIMPLE algorithm. The normalized residual values are converged at 10^{-5} for all variables. QUICK and central differencing flow numerical approaches have been implemented for convective and diffusive terms, respectively. Besides, researchers have implicitly applied the discretized nonlinear equations. The pressure–velocity coupling algorithm SIMPLE (Semi Implicit Method for Pressure-Linked Equations) was chosen to evaluate the pressure field. At the inlet, uniform velocity profile has been imposed. Impermeable boundary condition and 10% turbulence intensity at the inlet have been implemented over the channel wall while a constant heat flux condition is applied to over lower wall to create a thermally developed condition [2].

In this case two parameters have been presented, Friction factor and Nusselt number. Friction factor is calculated by pressure drop across the length of test section as [2]:

$$f = \frac{(\Delta p / L)D_h}{\frac{1}{2}\rho u^2} \qquad (15)$$

where D_h is hydraulic diameter, ρ and u are density and velocity, respectively. The local Nusselt number is defined by:

$$Nu(x) = \frac{h(x)D_h}{k} \qquad (16)$$

and average Nusselt number can be calculated by:

$$Nu = \frac{1}{l}\int Nu(x)dx \qquad (17)$$

IV. GRID TESTING AND CODE VALIDATION

Grid testing is implemented using several mesh sizing and densities to guarantee a grid independent solution. Air is used as a gird testing fluid with four different grids sizes of 30,225 cells, 51,050 cells, 94,050 cells, and 104,800 cells are selected to compare their local Nusselt numbers with the RNG k−ε turbulence model. Fig. 2 represents various local Nusset numbers of different grid sizes. The results revealed that after 94,050 cells, the difference between results is less than 4%. Therefore, mentioned grid size is chosen which separate the results dependence from grid size.
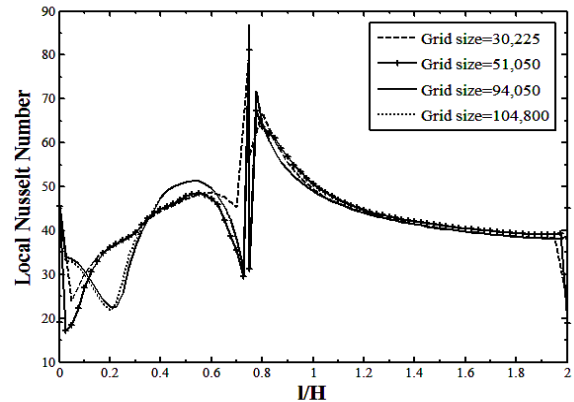

Fig. 2 Effect of grid size on local Nusselt number at Re=9000

Fig. 3 shows the accuracy of the selected grid size. The deviation of this study and referred study is slightly increased with the raise of Reynolds number. However, this percentage of deviation is less than 5% which can be evidenced that the results of the foregoing grid size are in accordance with Smith and Pongjet study [2].
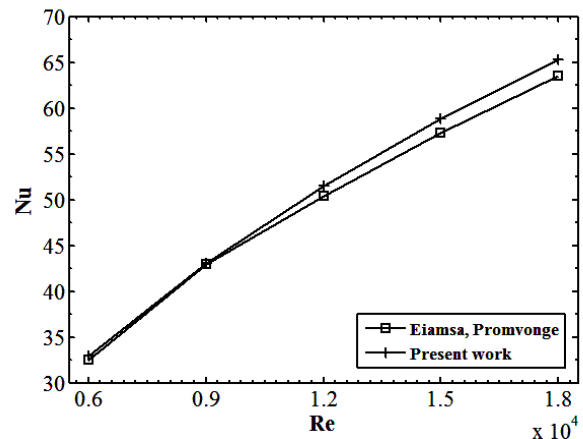

Fig. 3 Validation of local Nusselt numbers at different Reynolds number

V. RESULTS AND DISCUSSION

The simulations present three types of nanoparticles, SiO_2, AL_2O_3, and ZnO, and pure water. The values of nanoparticles volume fraction and diameter are in the range of $1\% \leq \phi \leq 4\%$ and $20nm \leq d_p \leq 50nm$ respectively. Water is considered as a base fluid of nanoparticles.

World Academy of Science, Engineering and Technology
International Journal of Mechanical and Mechatronics Engineering
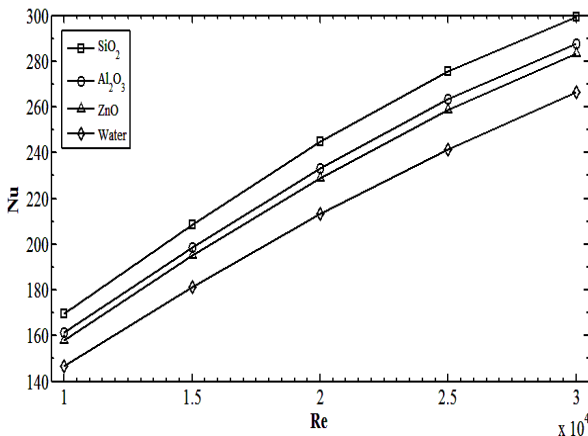Vol:6, No:12, 2012

Fig. 4 Effect of Reynolds number on the variation of the local
Nusselt number

Fig. 4 depicts the predicted results of average Nusselt number in a range of Reynolds number in the grooved channel by using the RNG k−ε turbulence model. In this case, nanoparticles are followed with a fixed nanoparticle diameter of 20nm and volume fraction of 4%. As can be seen in Fig. 4, the average Nusselt number increases with Raylonlds number increment for all types of nanofluids and pure water. Obviously, all of the nanofluids have a superiority comparison to pure water in average nusselt number over all ranges of Reynolds number. Also average Nusselt number of Al2O3 is reported slightly more than ZnO. It would be evident that SiO2 represents the maximum heat transfer due to considerable difference in average Nusselt number compared to above fluids.

Fig. 5 represents the influence of increasing the Reynolds number on friction factor. It would be obvious that the graphs almost coincided on each other which means that the friction factor difference can be overlooked for SiO_2, Al_2O_3, Zno, and water. Thus, it is founded that no or slight pressure loss is the cost of using nanofluids compared to the pure water in the case of pumping power. Moreover, the friction factor tends to decrease by increasing Reynolds number for all types of nanoparticles and pure water.
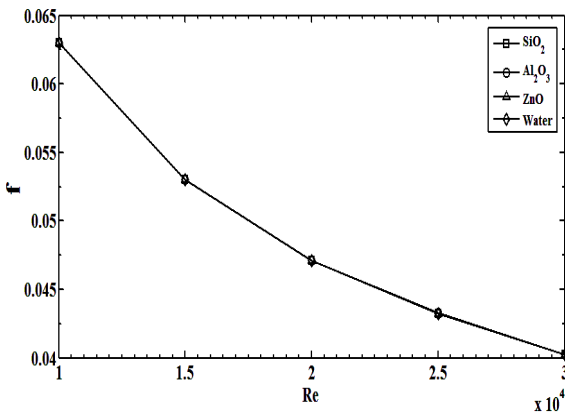

Fig. 5 Distribution of friction factor in a range of Reynolds number

The results indicate that the nanofluids have a higher average Nusselt number than water and also among them, SiO_2 could be an effective nanoparticle in the case of heat transfer enhancement due to the increment of the nanofluids and the particles densities in the thermal conductivity compared to the conventional fluids; the material with the lowest density has the highest Nusselt number.
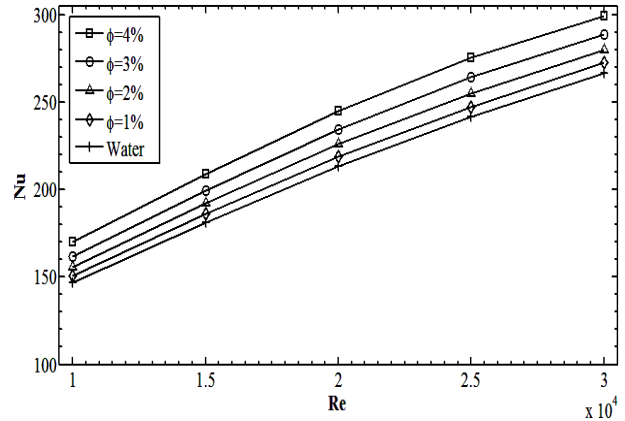

Fig. 6 Effect of volume fraction on Nusselt number of SiO2 at
different Reynolds number

According to the straight effect of ϕ on thermal conductivity in Eq. 12, changing this value has straightly affected on heat transfer enhancement. In this case, the influence of various volume fractions such as ϕ=1%, ϕ=2, ϕ=3%, and ϕ=4% on Nusselt number in SiO_2 nanoparticle at a range of Reynolds number in a fixed nanopaticles diameter (20nm) is shown in Fig. 6.

It would be obvious that Nusselt number increases with the rise in volume fraction in all ranges of Reynolds number. Volume fraction of 4% reveals considerable heat transfer enhancement in SiO_2 nanoparticle. By way of comparison, water is also trend the increasing Nusselt number as the Reynolds number increase but not as well as SiO2. Nanoparticle diameter is another characteristic of nanoparticle which generally affects on viscosity.

Fig. 7 illustrates the effect of changing SiO_2 diameter in four nanoparticle diameters values (d_p=20nm, d_p=30nm, d_p=40nm, and d_p=50nm) with a constant volume fraction of 4%. In spite of a considerable heat transfer enhancement compared to pure water for all values of nanoparticle diameter, the rise with the nanoparticle diameter has a negative efficacy on heat transfer enhancement due to inverse effect of nanoparticle diameter on a uniform velocity. Obviously, maximum heat transfer enhancement can be obtained by nanoparticle diameter and volume fraction of 20 nm and 4% respectively.
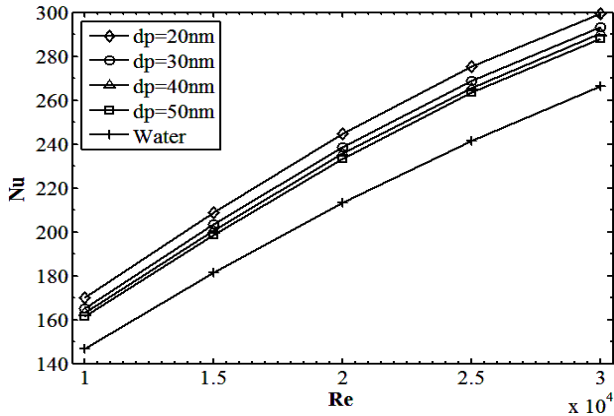
World Academy of Science, Engineering and Technology
International Journal of Mechanical and Mechatronics Engineering
Vol:6, No:12, 2012

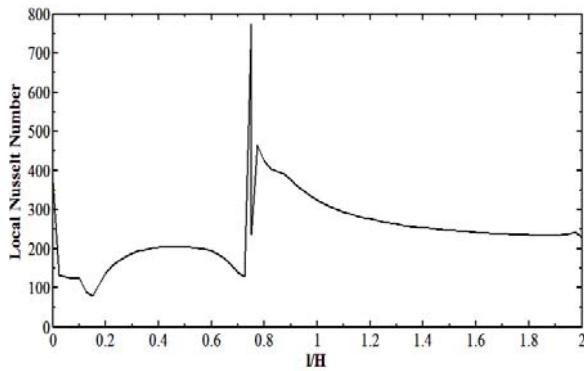Fig. 7 Effect of SiO_2 diameter on Nusselt number at different Reynolds number

Fig. 8 Local Nusslet number on fifth groove and rib

Indeed, local Nusselt number of first rib and groove considerably vary with the next pair of rib and groove, local Nusselt number of fifth rib and groove graph is chosen to remove this primary effect. In this case, Fig.8 shows local Nusselt number of SiO_2 with volume fraction of 4% and nanoparticle diameter of 20nm in the Reynolds number of 20000. A dramatically decrease on local Nusselt number is seen when the nanofluid comes to the left wall of the groove then a fluctuation on local Nusselt number can be observed in order to recirculation flow in the groove since then the graph has seen a dramatic rise due to impinging the flow to the rib wall which shows the effect of grooved channel on heat transfer by using nanoparticle more significantly.

VI. CONCLUSION

In the present investigation, a numerical simulation of 2-dimensional turbulent forced convection flow over periodic grooves in a horizontal channel heated by a uniform heat flux on grooved wall and insulated upper wall has been conducted in a Reynolds number range of 10000 to 30000 and B/H=0.75. RNG k−ε turbulence model has been chosen due to acceptable simulation of this model with experimental results at the similar condition. Variety types of nanoparticle and nanoparticle characteristics with water as base fluid have been chosen to identify the appropriate nanoparticle and its characteristics on heat transfer compared to the pure water.

Since constant friction factor has been reported almost for all types of nanoparticles, SiO_2 with 4% volume fraction and 20nm nanoparticle diameter provides highest heat transfer enhancement.

REFERENCES

[1] Ankit Kumar, A.K.D., Effect of a circular cylinder on separated forced convection at a backward-facing step. International Journal of Thermal Sciences,Vol. 52, p. 9, 2012.
[2] S.Eiamsa-ard ,P.Promvonge, Numerical study on heat transfer of turbulent channel flow over periodic grooves. International Communications in Heat and Mass Transfer, 35, pp. 844-852, 2008.
[3] T.Adachia, Y.Tashiroa, H.Arimab, Y.Ikegami(2009), Pressure drop characteristics of flow in a symmetric channel with periodically expanded grooves, Chemical Engineering Science, vol.64, pp. 593—597, 2009.
[4] T.Adachi, H.Uehara , Correlation between heat transfer and pressure drop in channels with periodically grooved parts, International Journal of Heat and Mass Transfer, vol. 44, 2001.
[5] S.Eiamsa-ard, P.Promvonge, Thermal characteristics of turbulent rib-grooved channel flows, International Communications in Heat and Mass Transfer, vol. 36, pp. 705–711, 2009.
[6] J R. Kamali ,A.R. Binesh, The importance of rib shape effects on the local heat transfer and flow friction characteristics of square ducts with ribbed internal surfaces, International Communications in Heat and Mass Transfer, vol. 35, pp. 1032–1040, 2008.
[7] H.Shokouhmand ,K.Vahidkhah, M.A.Esmaeili, Numerical Analysis of Air Flow and Conjugated Heat Transfer in Internally Grooved Parallel-Plate Channels, World Academy of Science, Engineering and Technology, vol. 73, 2011.
[8] M.Greiner, F,Fischer,M.Tufo, Two-Dimensional Simulations of Enhanced Heat Transfer in an Intermittently Grooved Channel, Journal of Heat Transfer, Vol. 124, June 2002.
[9] M C. Herman, E. Kang , Comparative evaluation of three heat transfer enhancement strategies in a grooved channel, Heat and Mass Transfer, vol. 37 , pp.563-575, 2001.
[10] L.Ortiz, A. Hernandez-Guerrero, C. Rubio-Arana, R. Romero-Mendez, Heat transfer enhancement in a horizontal channel by the addition of curved deflectors, International Journal of Heat and Mass Transfer, vol. 51, pp. 3972–3984, 2008.
[11] Oronzio Manca, S.N., Daniele Ricci, A numerical study of nanofluid forced convection in ribbed channels. Applied Thermal Engineering,vol. 37, pp. 280-292, 2012.
[12] A.A. Al-aswadi, H.A.M., N.H. Shuaib, Antonio Campo, Laminar forced convection flow over a backward facing step using nanofluids. International Communications in Heat and Mass Transfer, vol 37, 2010.
[13] S. A. Sh. Kherbeet , H.A.M., B.H. Salman, The effect of nanofluids flow on mixed convection heat transfer over microscale backward-facing step. International Journal of Heat and Mass Transfer, 2012.